18th International Conference on Protection & Automation in Power System
Shahrood University of Technology
January 9, 2024 - January 10, 2024

Fault Detection and Classification in Parallel and semi-parallel Transmission Lines Connected to Large-Scale Photovoltaic Power Plants Using Artificial Neural Networks and Support Vector Machines

Alireza Jodaei
Faculty of Electrical & Computer Engineering,
Semnan University, Semnan, Iran
a.jodaei@semnan.ac.ir

Zahra Moravej
Faculty of Electrical & Computer Engineering,
Semnan University, Semnan, Iran
zmoravej@semnan.ac.ir

Mohammad Pazoki
School of Engineering,
Damghan University, Damghan, Iran
pazoki.m@du.ac.ir

***Abstract*—Sustainable energy supply and the increasing use of large-scale photovoltaic power plants (LSPPPs) demand stronger and more reliable transmission systems. Parallel transmission lines are widely employed in modern power systems to enhance the reliability and security of electrical energy transmission. With the need for energy transfer from LSPPPs and the impact of LSPPPs of changing the nature of faults, parallel transmission lines face new challenges. This paper investigates the detection and classification of faults with various characteristics in parallel and semi-parallel transmission lines using Artificial Neural Networks (ANNs) and Support Vector Machines (SWM). This approach facilitates the enhancement of efficiency and confidence in transmission systems and contributes to organizing stable and reliable performance in these systems. For simulation and analysis, the PSCAD/EMTDC software is employed to simulate the model of parallel and semi-parallel transmission lines connected to LSPPPs. Subsequently, the three-phase current signal values and the positive sequence voltage angle signals of the two buses connected to the transmission line are extracted, processed, and divided into training and testing data using MATLAB software. Then, these two methods have been compared. The results demonstrate that ANN and SWM are capable of accurately detecting and classifying faults with high precision.**

Keywords- Parallel transmission line, Protection of transmission line, Distance protection, Large-scale photovoltaic power plants, Artificial neural network, Support Vector Machines.

I. Introduction

A. *Motivation and incitement*

Renewable energy generation is rapidly increasing worldwide to meet the growing demand for electrical energy in society. The introduction of LSPPPs has introduced challenges, such as maloperation of transmission line protection systems [1]. Inverters play a crucial role in connecting LAPPP to power systems, differentiating them from traditional synchronous generators (SGs) and LSPPPs [2]. This shift has compelled researchers to adapt traditional approaches for calculating short-circuit (SC) currents [3]. As demonstrated in [3], the integration of renewable power plants like LSPPPs into the grid alters the impedance path detected by distance relays compared to that associated with conventional generation sources. On the other hand, the increasing demand for electrical energy necessitates effective operations in energy supply and transmission to maintain power system security. Parallel transmission lines are favorable choices for integrating electrical transmission systems as they provide greater transmission capacity over existing access routes [4].

B. *Literature review*

The effectiveness of protection systems has been extensively investigated in various papers. In [5], a two-stage protection scheme based on machine learning is proposed, where the proposed algorithm provides fault classification in the first stage for a transmission line connected to a wind farm and fault identification and location capabilities for distance relays in the second stage. In [6], challenges related to wind power plants during network disturbances and their impact on transmission

line protection systems are presented. This study introduces an artificial intelligence-based protection method that utilizes Variational Mode Decomposition (VMD) and Deep Convolutional Neural Network (CNN) techniques for fast and effective fault detection and classification. The use of VMD for feature extraction from network-side current signals and CNN for fault classification is applied. The performance of distance relays, widely used in transmission line protection, is influenced by the connection of parallel lines. Various impedance-based algorithms exist for compensating mutual coupling effects [7, 8], assuming that the source impedances on both sides of the line are the same. This assumption does not hold true for a system connected to LSPPPs. In [9], a method for protecting parallel lines with series compensations in the presence of solar power plants is introduced, utilizing the positive sequence components of current and voltage. In this approach, faults are detected using criteria derived from the phase angle between the difference in line current and pre-fault voltage. One of the most common techniques in artificial intelligence for fault analysis is the use of Artificial Neural Networks (ANN). ANNs are widely used in electrical engineering for prediction, estimation, modeling, control, signal processing, and pattern recognition. The ability of ANNs to learn complex systems, makes them suitable for modeling systems that cannot be easily mathematically modeled. In [10], an adaptive protection scheme aimed at enhancing the performance of distance protection by combining ANN and fault resistance calculations is proposed. In [11], an innovative ANN-based fault location algorithm is introduced for distribution feeders. This algorithm harnesses phasor measurements of voltage and current at the substation to provide precise fault location estimates. Extensive simulations carried out on the IEEE 34 feeder test system showcase the ANN's remarkable accuracy in estimating fault locations across a broad spectrum of fault resistances. Furthermore, in [12], a combined approach using wavelet transforms and ANN for fault classification in the series-compensated transmission lines is reported. The challenge of fault detection and classification in the series-compensated EHV transmission lines is addressed using a hybrid wavelet-ANN protection scheme in [13]. In [14], a comprehensive exploration of the challenges associated with safeguarding power transformers is presented. The paper introduces an innovative ANN-based algorithm designed for the recognition of current waveforms in transformer protection. In [15], fault detection and classification in transmission lines using Discrete Wavelet Transformation (DWT) for three-phase current signals are proposed. ANN, k-NN, and DT classifiers are employed for fault classification, with ANN achieving 100% accuracy as the best-performing algorithm. However, this study does not consider the presence of LSPPP. In [16] utilized the Support Vector Machine (SVM) technique for fault detection, and the ANN technique for fault location and classification in a 400 kV three-phase double-circuit transmission line under both linear and non-linear load conditions, achieving improved accuracy. In [17], a proposed algorithm based on ANN and SVM is presented for fault detection and classification in transmission lines connected to wind power plants. In [18], a novel differential protection and condition monitoring scheme for power transformers utilizing ANNs is introduced. This ANN-based scheme demonstrates remarkable accuracy in detecting internal faults and promptly issuing trip signals. The authors employ two distinct ANN structures, one for fault detection and another for condition monitoring. To train these ANNs effectively, they utilize the Radial Basis Function (RBF) learning algorithm.

C. Contribution and organization

Despite the advantages offered by previous approaches, most studies have either focused on simple transmission lines or only examined parallel transmission lines connected to two common buses. However, in some cases, such as the proximity of large power plants and urban areas, transmission lines are partially coupled as they are located at a specific distance in a common bus and terminate in different buses. In this paper, the impact of LSPPP connection on the performance of distance protection is investigated under various scenarios, including cases where transmission lines are completely parallel or conditions where semi-parallel transmission lines are also used, for faults with different characteristics. Subsequently, the ANN and SWM methods have been employed for the identification and classification of various types of faults. The main innovations and contributions of the proposed paper are:

- Investigation of the Impact of Parallel and Semi-Parallel Transmission Lines on the Performance of Distance Protection in the Presence of LSPPP: This study delves into the influence of parallel and semi-parallel transmission lines on the functionality of distance protection relays when integrated with LSPPP. It examines the unique challenges posed by these configurations, shedding light on their effects on fault detection and relay operations.
- Utilization of ANN and SWM for Fault Identification and Classification in the Scenarios Described in Point 1 to Enhance Distance Protection Performance: To address the challenges highlighted in the first contribution, this paper employs ANN and SWM as an advanced tool for accurate fault identification and classification. The integration of ANN and SWM in distance protection schemes aims to improve the overall reliability and effectiveness of the protection system. Then, these two methods have been compared.
- High Precision in Identifying and Classifying Various Types of Faults Considering Different Fault Resistances and Locations: This research achieves remarkable precision in the identification and classification of diverse fault types. It takes into account variations in fault resistances and fault locations, providing a comprehensive and reliable approach to fault detection and classification in power transmission systems.

These contributions collectively advance the field of power system protection, particularly in the context of LSPPP integration with parallel and semi-parallel transmission lines, showcasing the potential for enhanced reliability and performance in modern power grids.

The paper is structured into six sections. Section II introduces a problem statement. In Section III, the ANN method is outlined. Section IV, the SWM method is outlined, Section V, dedicated to presenting the performance results of the proposed algorithm. Finally, Section VI provides the conclusion.

II. Problem statement

The fault current from the SG source exhibits substantial amplitude and uncontrollable characteristics. As depicted in Fig. 1, within a power system in connected to LSPPP interconnected via a DC link, the integration of a capacitor notably mitigates the impact of fault dynamics. While the fault response time remains remarkably rapid, the intermittent response tends to exhibit a more gradual nature. Consequently, the inverter plays a pivotal role in shaping the dynamic response of LSPPP during faults, with its activation time heavily reliant on the responsiveness of power system control mechanisms. The primary control system for fault management relies on data collected at the point of common coupling (PCC), encompassing voltage and current measurements. Additional variables that influence this current include the electrical characteristics of the power source and short-circuit impedance. In contrast, PV fault currents exhibit relatively lower amplitudes and are susceptible to changes based on the control strategy employed for switching power electronic devices. In conventional systems, relay settings are calibrated based on high-amplitude short-circuit currents and inductive effects arising from synchronous generators (SG). However, as PV penetration increases and fault current characteristics evolve, the risk of the protection system's misoperation also rises. Signals directly affected by LSPPP can be categorized into three distinct periods. In the initial phase, there is a peak in the short-circuit (SC) current, depending on the filter characteristics and the DC link capacitor. This peak may reach magnitudes exceeding a few per unit relative to the inverter's base rating. The second phase involves regulation, where the inverter control system actively stabilizes the DC link voltage. This is done to ensure current compliance with grid codes (GC), meet fault ride-through (FRT) requirements, and limit the peak of the SC-current. Finally, in the third phase, the inverter output current and voltage attain and maintain an almost constant level. Consequently, the behavior of LSPPP deviates from the conventional pattern and can be described as a function of fault conditions, system configurations, and the parameters governing its control system [19].

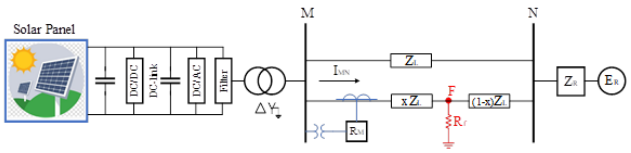

Fig. 1. Transmission network in the presence of LSPPP.

Inverters possess a crucial capability to control fault currents, allowing for the manipulation of phase angles within the fault signal, irrespective of the fault's inherent characteristics. Additionally, while the synchronous generator (SG) system typically exhibits an inductive response, inverter control can manifest as inductive, capacitive, or resistive behavior. Consequently, these variations in behavior may lead to several implications, including inaccuracies in impedance measurements, discrepancies in the comparison of positive and negative-sequence phase angles, variations in phase angle assessments for individual phases, fluctuations in phasor current signals at the extremities of transmission lines, and alterations in the relationship between polarized and operational parameters. Traditionally, negative-sequence parameters have served as the primary protective measures, with an aim to reduce reliance on zero-sequence parameters. Consequently, changes in negative-sequence current induced by LSPPP may result in a breakdown in directional supervision, ultimately leading to the deactivation of distance protection elements. Historically, Mho relays have been the linchpin of transmission line protection for detecting various fault types. Nevertheless, the integration of LSPPP modifies fault characteristics, thereby increasing the likelihood of malfunctions in the protection system [5].

A. Measured distance protection on parallel lines

The primary challenge encountered by traditional distance relays when deployed in parallel transmission lines stems from the mutual coupling effect between the lines. This effect exhibits variability contingent upon the operational and fault conditions of the lines.

Conventional distance relays were originally devised with a primary focus on single-line distance protection applications. In the event of a fault transpiring on a solitary line, the impedance observed by the conventional distance relay is directly related to the distance between the relay and the fault location. This relationship is established through the utilization of the conventional zero-sequence current compensation method for LG faults (equation 2). In equation 3, the impedance value measured by the distance relay when LL, LLG, LLL and LLLG faults occur is shown [6].

$$Z_{app} = \frac{V_{rM}}{I_{rM}} = \mathrm{x}Z_{1L} + \left(\frac{I_f}{I_{rM}}\right)R_f \quad (1)$$

$$\frac{V_{rM}}{I_{rM}} = \frac{V_{LG}}{I_L + K_0 I_0} \quad ,K_{0L} = \frac{Z_{0L} - Z_{1L}}{Z_{1L}} \quad (2)$$

$$\frac{V_{rM}}{I_{rM}} = \frac{V_{LL}}{I_{L1} + I_{L2}} \quad (3)$$

Where, V_{rM} and I_{rM} represent the operating voltage and current for the relay R_M, respectively, K_0 is the line zero sequence current compensation factor; Z_{0L} and Z_{1L} are the zero and positive sequence impedance of the line; x is the per-unit distance between the relay and the fault location. In the context of protecting parallel transmission lines, as depicted in Fig. 1, the application of a conventional distance relay leads to inaccuracies in distance measurements. These inaccuracies primarily stem from the cross-coupling effect between parallel lines and the presence of LSPPP. In general, the mutual coupling effects resulting from positive and negative sequence currents between parallel lines are minimal and can be considered negligible. Therefore, considering Equation 3, parallel lines have no impact on the measured impedance during LL, LLG, LLL, LLLG occurrences. Nevertheless, it's essential to note that the mutual coupling effects of zero sequence currents between parallel lines may be significant. The calculated apparent impedance (Z_{app}), by the distance relay situated at bus M (R_M) in the event of an LG fault with a fault impedance of R_f, is determined as per the equation (4). As illustrated in Fig. 2, the computation of Z_{app} takes into account the intricate interplay of voltage, current, and network parameters at the relay's location.

This computation holds a critical role in assessing the condition and performance of the electrical grid, serving as a key factor in optimizing the operation of the transmission lines. Furthermore, in the presence of varying network conditions and potential oscillations, the precise analysis of Z_{app} facilitates proactive measures to prevent potential incidents and faults within the power transmission system. These enhancements contribute significantly to the overall stability and reliability of the electrical grid.

$$Z_{app} = \frac{V_{LG}}{I_L + K_0 I_0} = xZ_{1L} + \Delta Z_{Parallel} + \Delta Z_{LSPPP}$$
$$\Delta Z_{Parallel} = \frac{x\left(Z_{M0}\right) * I_{PL0}}{I_L + K_0 I_0}, \quad \Delta Z_{LSPPP} = \frac{R_f * I_f}{I_L + K_0 I_0} \tag{4}$$

In (3), Z_{M0} is the total zero sequence mutual coupling line impedance and I_{PL0} is the parallel line's zero sequence current. As depicted in (1), the Z_{app} is calculated by summing the impedance values of the line from bus M to the faulted point, along with two variable impedances $\Delta Z_{parallel}$ and ΔZ_{LSPPP} that depends on network-specific variables. The magnitude of $\Delta Z_{parallel}$ is contingent upon the total zero sequence mutual coupling line impedance and parallel line's zero sequence current [7]. The magnitude of ΔZ_{LSPPP} is contingent upon the ratio of $\frac{I_F}{I_{rM}}$ and the fault resistance. Conversely, one of the distinctive attributes of converters employed in LSPPP is their capability to limit fault current. The limitation of fault current by the LSPPP interfacing converters causes the ratio $\frac{I_F}{I_{rM}}$ to be significantly higher compared to a conventional power network with synchronous generator-based sources. This alteration leads to a substantial disparity between Z_{MF} and Z_{app} in the presence of LSPPP [8]. The control scheme employed in LSPPP is of paramount importance in determining both the reduction of fault current and the phase angle value. The phase difference between (I_F) and (I_{FrM}) is contingent upon the phase angle of the fault current, and as this phase angle undergoes variations, the disparity between them significantly increases. Consequently, these variations result in the introduction of an additional reactance to ΔZ_{LSPPP}. This added reactance shifts the apparent impedance along the imaginary axis within the R-X plane.

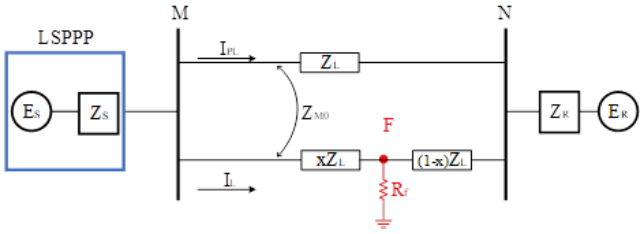

Fig. 2. Parallel line system

B. semi-parallel transmission lines

Previous approaches have primarily focused on parallel transmission lines, which originate and terminate at the same substation. In such scenarios, these lines exhibit full coupling, allowing data from adjacent lines to be easily accessible at both ends. However, it is crucial to recognize that there are specific situations, particularly in the proximity of large-scale power plants or urban areas, where transmission lines experience only partial coupling. In these instances, multiple lines may share the same tower within a certain proximity but terminate at different substations. It is worth mentioning that transmission lines may temporarily follow distinct paths away from a substation due to considerations related to system reliability. However, this temporary divergence typically occurs over a short distance before the lines reconverge, often sharing the same tower. This configuration is frequently encountered with double-circuit or multi-circuit transmission lines. These variations in line coupling and topology introduce unique challenges and considerations when it comes to fault detection and protection. Figs. 3 and 4 illustrate scenarios involving partially coupled transmission lines that do not terminate at the same substation, which is considered the distance value of this part y. In these figures, transmission lines MN and MS share a common tower up to point D, resulting in mutual coupling between them. In the event of a fault occurring on line MN, the zero-sequence currents in both lines MN and MS may flow in different directions. This divergence in current flow can lead to an over-reach condition for relay R1. In the proposed plan for calculating the impedance seen by the relay in bus M, two scenarios can be considered according to the fault location:

a. The location of the fault between the MD line

In this scenario, the location of the fault is considered between two points M and D of the line, or in other words, the fault occurred in the parallel part of the line ($\frac{y}{x} > 1$). In this situation, if a hypothetical bass is considered at point D, the schematic of Fig. 3 (a) can be considered similar to Fig. 2, so it can be said that relation 4 is also true for this situation.

b. The location of the fault between the DN line

In this scenario that shows in Fig. 3 (b), the location of the fault is considered between two points D and N. In other words, in this condition, $\frac{y}{x} < 1$. In this situation, considering that the parallel part of the two circuits is less than the distance between the fault location and the relay, so relation 4 is not correct for this situation. The influence of the parallel part of the system on the impedance seen by the relay can be expressed as equation 5.

$$Z_{app} = \frac{V_{LG}}{I_L + K_0 I_0} = xZ_{1L} + \Delta Z_{Parallel} + \Delta Z_{LSPPP}$$
$$\Delta Z_{Parallel} = \frac{y\left(Z_{M0}\right) * I_{PL0}}{I_L + K_0 I_0}, \quad \Delta Z_{LSPPP} = \frac{R_f * I_f}{I_L + K_0 I_0} \tag{5}$$

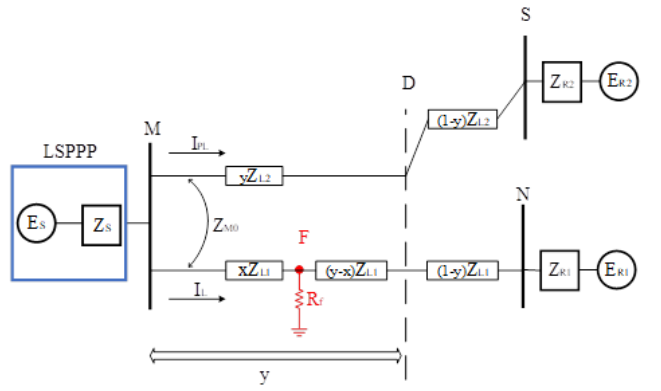

(a)

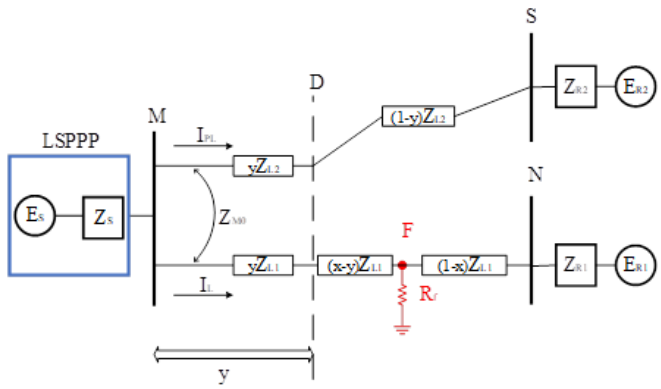

(b)

Fig. 3. semi-parallel transmission lines with fault occurring in (a) MD and (b) DN

III. Artificial Neural Network Technique (ANN)

The human brain is an intricate organ composed of millions of neurons, each responsible for performing intricate tasks. It receives signals from various parts of the body and, through complex processes within the brain, generates appropriate responses naturally. ANNs operate on a similar principle but are artificial constructs. ANNs possess several key capabilities, including parallel processing, nonlinear mapping, and both online and offline learning approaches. In artificial systems, neurons are referred to as nodes, and ANNs are typically structured with an input layer, hidden layers (if applicable), and an output layer. The specific configuration of an ANN, known as its network topology, plays a crucial role in its functionality. Network topologies can include feedforward architectures, whether single-layer or multi-layer, as illustrated in Fig. 4, or feedback networks for processes such as weight updating and learning. These characteristics enable ANNs to simulate and perform tasks akin to those of the human brain, making them valuable tools in various applications [9]. The flowchart of the SVM Classifier algorithm is shown in Fig. 5.

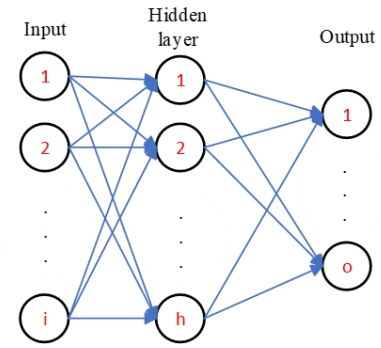

Fig. 4: ANN topology

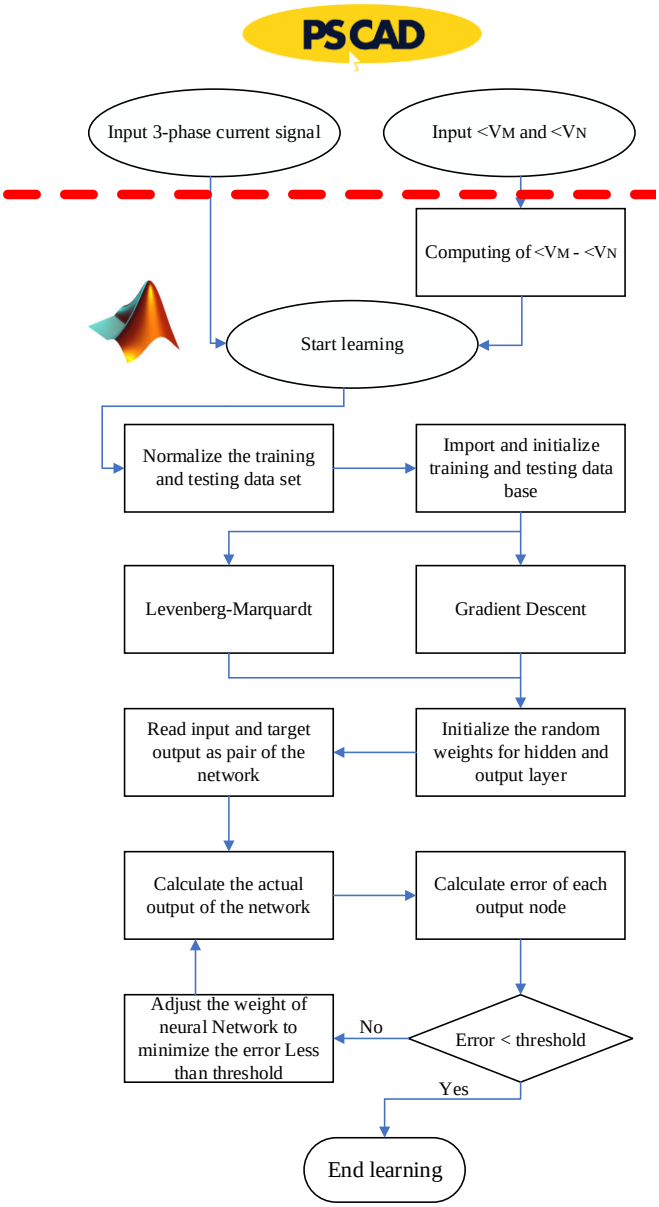

Fig. 5. Flowchart of the ANN Training Model.

IV. Support Vector Machine (SVM)

SVM is a statistical technique used for computational learning, offering several advantages over ANN. SVM provides a global solution rather than getting stuck in local minima, which can happen with ANN. SVM classifiers are known for their high accuracy and efficiency in handling high-dimensional data. They are memory-efficient because they use a subset of training points during validation [24]. SVM classifiers can be employed in various ways, including:

- Binary Classifier: SVMs can serve as binary classifiers, distinguishing between two classes, such as in-zone faults (+1) and no faults (-1).
- Multi-layer Classifier: SVMs can also be used as discrete classifiers, particularly suited for regression problems.

The primary objective of SVM classifiers is to create a boundary or hyperplane that maximizes the margin between different class labels. This hyperplane is represented by equation (6).

$$f(x) = W^T . x + b = 0 \quad (6)$$

Where, W is weight vector and b is a bias term to determine position of hyper-plane. Cost (C) and Gamma (γ) serve as critical hyper-parameters, and they are configured prior to training the model. Hyper-parameters play a crucial role in error control and determine the curvature weight of the decision boundary. A small value of C results in a wide margin, leading to numerous support vectors and a higher number of misclassified observations. Conversely, a larger C value results in a narrower margin, reducing the number of support vectors and misclassified data points. It's worth noting that a lower cost (C) value generally improves the performance on test datasets and helps prevent overfitting [10]. The flowchart of the SVM Classifier algorithm is shown in Fig. 6.

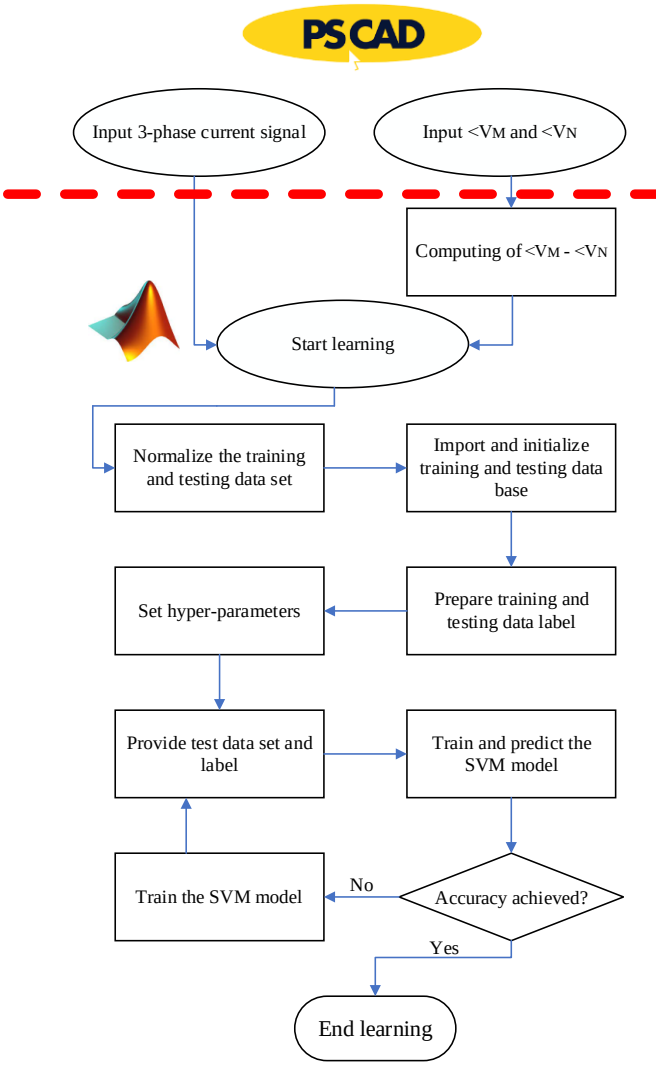

Fig. 6. Flowchart of SWM

V. Simulation result

In this section, the simulation results for the system illustrated in Fig. 1 are presented. Table I provides an overview of the system data for a partially coupled transmission line. The transmission lines originating from Bus M in Fig. 1 and terminating at Buses N each span a length of 200 km. Line impedances are expressed in Ohms per km, allowing us to investigate various coupled lengths, in simulation studies [7]. A 100 MW PV plant with a double-stage connection to bus M through a dYg1 transformer, as shown in Fig. 1, is employed to optimize the PV plant's power output using MPPT in the boost converter [4]. The power system is simulated using the PSCAD/EMTDC environment, while the proposed algorithm is implemented in MATLAB.

A sampling frequency of 3.2 kHz was employed, corresponding to the 60 Hz nominal frequency. Post-fault data were captured using measuring devices such as CVT and CT, which is a standard configuration commonly found in digital relays available in the market. Simulations were conducted for all eleven types of faults occurring on the line between bus M and bus N, considering various fault locations and different values of fault resistance. For each case, data files were generated by measuring and recording the three-phase current signal values at bus M and the positive sequence voltage angle signals of the two buses connected to the transmission line using PSCAD software. Then, the difference of these two angles is calculated as sample data. The sampled data are given as input to the ANN and SVM algorithms for training, and the trained model is used for testing purposes.

Table 1: Simulation system parameters

Parameters	Values
Transmission line length	200 km
Nominal voltage	230 kV
Positive sequence impedance	$0.36855\angle 84.97\ \Omega$/km
Zero-sequence impedance	$1.4149\angle 82.88\ \Omega$/km
Zero-sequence mutual impedance	$0.9596\angle 80.6\ \Omega$/km
Equivalent positive sequence impedance	$20.22\angle 81.46\ \Omega$
LSPPP	Number of PV arrays & cells in series per module: 130, 35, irradiance: $1000^{W}/_{m^2}$, Temperature: 25 °c, KP = 0.15 & Ti = 0.08 s, DC Link capacitor: 7800 μF , L_f = 300 μF , C_f = 200 μF , R_f = 0.025Ω.

Fig. 7 shows the measured impedance values for different states of the system. These modes have been investigated according to the occurrence of LG fault with $R_f = 10\ \Omega$ and x=100 km. In this Fig, the impedance values seen by the distance relay are depicted using different colors to illustrate various scenarios. The orange line represents the impedance value observed in a single-circuit line, assuming that the source is connected to bus M in the SG system. Moving to the yellow line, it shows the impedance value measured when the system becomes a two-circuit configuration, but the source, connected to bus M, is still assumed to be SG. Notably, the two-circuit line leads to an increase in the calculated impedance value, as indicated by the yellow line. The purple line in Fig. 7 represents the impedance value seen by the relay in the case where the double-circuit line is connected to LSPPP at bus M. This particular impedance exhibits a significant change compared to the previous values, which could potentially result in a malfunction of the protection system, deviating from conventional expectations. This observation underscores the need for further investigation and adaptation of protection schemes in the presence of LSPPP.

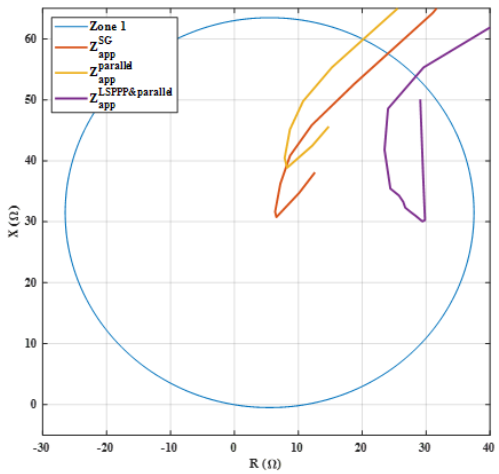

Fig. 7. Measured impedance values for different states of the system

Fig. 8 shows the difference in the impedance seen by the distance relay in bus M for the systems shown in Figs. 3a and 3b. These modes have been investigated according to the occurrence of LG fault with $R_f = 10\ \Omega$ and x=80 km. In the first case, a value of y =100 km and in the second case, a value of y =60 km is considered. Considering that in Fig. 3a, the fault occurred in the parallel part of the circuit, it can be said that the effect of the parallel circuit on the measured impedance is not dependent on the value of y, and the effect of the parallel part is determined by the value of x. But in Fig. 3b, due to the fact that part of the circuit of the fault current path is parallel and part of it is single circuit, so the value of the parallel path has an effect on the measured impedance. Therefore, in this case, the value of y affects the observed impedance.

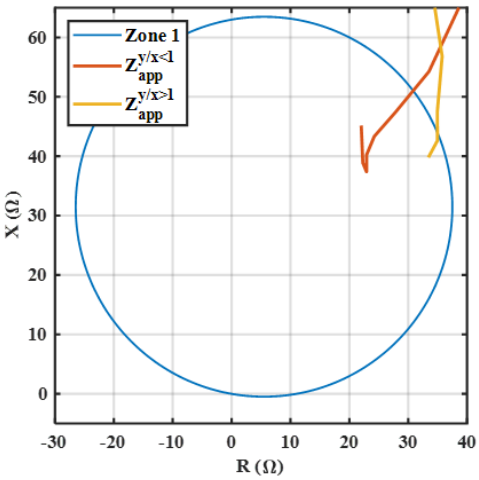

Fig. 8. Measured impedance values for different fault value of the parallel path

According to Fig. 8, the probability of wrong operation when the fault occurs is higher in the condition that the system is $\frac{y}{x} > 1$, so in order to check the effect of the fault resistance on the measured impedance, the sample system in Fig. 3b is taken into consideration and the results of the investigation in Fig. 9 can be seen.

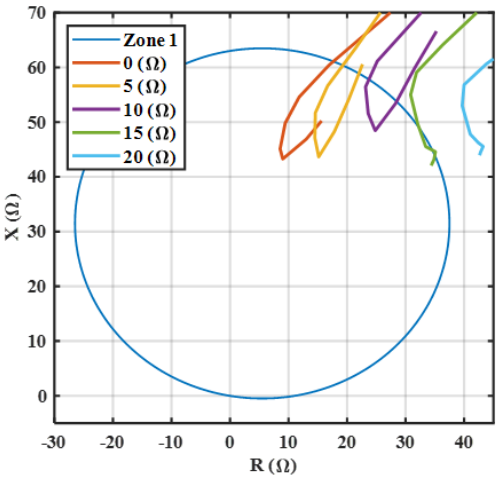

Fig. 9. Measured impedance values for different fault resistance

Table 2 shows different cases of 1098 faults created, respectively. It is observed from Tab. 1 that out of 1089 faults 495 (45.45 % of total cases) have been utilized as a training process of ANN and CNN. The remaining 594 (54.55 % of total cases) have been utilized for testing and validation of the proposed algorithm. The trained ANN and CNN based fault classifier models are then extensively used for testing of unseen fault data. The ANN and CNN fault detection technique have been verified for all symmetrical and asymmetrical faults (L-G, LL, LL-G, LLL, LLL-G) at different locations and different fault resistance.

Table 2: different cases of 1098 faults

Power system parameter	ANN/SWM training patterns		ANN/SWM unseen testing patterns	
	Variation in parameter	Numbers of variation	Variation in parameter	Numbers of variation
Fault type	LG-LL-LLG-LLL-LLLG	11	LG-LL-LLG-LLL-LLLG	11
Fault resistance (Ω)	0, 10, 20, 50, 100	5	1, 5, 15, 35, 75, 110	6
Fault location (y=100 km) (km)	10, 30, 50, 70, 90, 110, 130, 150, 170	9	15, 35, 55, 75, 95, 115, 135, 155, 175	9
Total (1089)	Total training patterns for fault	495	Total testing patterns for fault	594

A. ANN and SWM Technique Result

The ANN Backpropagation model was trained using various MATLAB functions. Table 3 presents the fault classification accuracy with 4 hidden layers, employing different training functions available in MATLAB. The choice of the training function depends on various factors, including the problem's complexity, the size of the training dataset, the number of weights and biases in the network, the number of hidden layers, the error goal, and whether the network is used for pattern recognition or regression tasks. Table 3 displays the fault classification accuracy for faults achieved by Gradient Descent, and Levenberg-Marquardt backpropagation training functions. Levenberg-Marquardt is the fastest backpropagation algorithm and provides better accuracy compared to the other backpropagation algorithm. The accuracy of identifying various faults using the Levenberg-Marquardt backpropagation training function increases with an increase in the number of hidden layers, as shown in Tables 4 for faults, respectively. Table 5 presents the accuracy of fault detection on the test dataset using the SWM Technique, which was not part of the training dataset and was achieved through MATLAB programming.

Table 3: Classification regression accuracy for different faults

Back propagation training function	Accuracy train (%)	Accuracy test (%)	Accuracy valid (%)
Gradient Descent	97.1	96.3	94.9
Levenberg-Marquardt	98.7	98.1	96.9

Table 4: Fault detection accuracy for different faults with ANN technique

Fault type	Number of test case	True	False	Accuracy (%)
LG	162	161	1	99.4
LL	162	162	0	100
LLG	162	160	2	98.7
LLL	54	54	0	100
LLLG	54	52	2	98.7
Total	594	589	5	99.15

Table 5: Fault detection accuracy for different faults SWM technique

Fault type	Number of test case	True	False	Accuracy (%)
LG	162	160	2	98.7
LL	162	161	1	99.4
LLG	162	162	0	100
LLL	54	54	0	100
LLLG	54	53	1	98.2
Total	594	590	4	99.32

In Fig. 10, the performance curve of the proposed model during the training process is presented. The vertical axis represents the cross entropy, which is a measure of the model's performance in minimizing the error between predicted and actual values. The horizontal axis represents the number of training epochs, where each epoch corresponds to one complete iteration through the training dataset. The curve illustrates the change in cross entropy on the validation dataset over multiple epochs. Notably, it can be observed that the validation performance reaches its best value at epoch 5, with a remarkably low cross entropy of 0.0093429. This point represents the model's highest level of accuracy and efficiency in predicting the desired outcomes. Furthermore, it is important to highlight that the behavior of the training, validation, and test curves in Fig. 10 is consistent throughout the training process. This uniformity indicates that the model generalizes well from the training data to both the validation and test datasets, reducing the risk of overfitting. Overfitting occurs when the model memorizes the training data but struggles to perform well on new, unseen data. In such cases, the validation error would typically increase while the training error decreases, which is not observed here. The findings from this performance analysis demonstrate the model's ability to effectively learn from the training data, generalize to

new data, and achieve outstanding results, as evidenced by the exceptional validation performance at epoch 5.

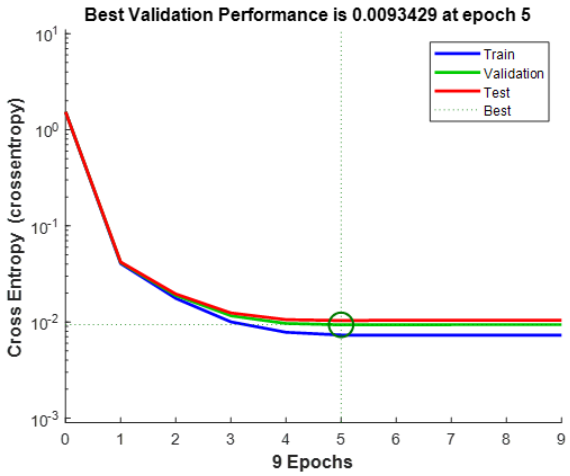

Fig. 10. Best validation performance error vs. epochs.

VI. Conclusions

In this paper, the effect of the presence of LSPPP on the protection of the transmission line of the two-circuit system has been investigated, and the possible topologies for parallel and semi-parallel transmission lines have been discussed, with the performance of distance protection in these types of systems being studied. Also, the impedance relationships Calculated by the distance relay in the indicated conditions, obtained. Then, an ANN and SVM-based fault discrimination scheme has been tested in the presence of LSPPP. The three-phase current signal and the positive sequence voltage angle signals of two buses connected to the transmission line are sampled. Then, the difference of these two angles is calculated as sample data. The sampled data are given as input to the ANN and SVM algorithms for training, and the trained model is used for testing purposes. The feasibility of the proposed scheme was evaluated in 594 test cases with varying fault conditions. The results indicate that the proposed scheme achieved a discrimination accuracy of more than 99.1% when using the ANN technique with 4 hidden layers in the MATLAB development tool. Additionally, the SVM technique yielded an accuracy of more than 99.3% with faster convergence time compared to the ANN method. Both methods proved to be simple, fast, and accurate for fault classification. In conclusion, the machine learning approaches employed in this study demonstrate excellent performance on the same test dataset.

- Both algorithms are parametric, with ANN parameters including the number of hidden layers, learning rate, activation function, number of iterations, and threshold error, while SVM parameters include kernel function gamma and margin parameter C.
- ANN and SVM classification approaches provide comparable accuracy and reliability depending on the training data.
- The ANN-based algorithm requires a trial-and-error process to determine the number of layers, neurons, and activation functions, making the overall design process complex. The ANN is considered a learning-based approach.
- SVMs can perform well with both small and large training datasets because the maximum margin boundary condition determines accuracy. In contrast, if a large or sufficient dataset is not provided to the ANN, it may result in poor classification.
- The training algorithm in SVM is faster compared to ANN. ANN training processes can be complex for high-dimensional problems, and the ANN may offer slow convergence in the backpropagation algorithm. Convergence depends on the initial selection of weight constraints.

References

[1] R. Salazar-Chiralt et al., "Dynamic interactions in large scale photovoltaic power plants with frequency and voltage support," Electric Power Systems Research, vol. 207, p. 107848, 2022.

[2] T. Kauffmann et al., "Short-circuit model for type-IV wind turbine generators with decoupled sequence control," IEEE Transactions on Power Delivery, vol. 34, no. 5, pp. 1998-2007, 2019.

[3] A. Jalilian, K. M. Muttaqi, D. Sutanto, and D. A. Robinson, "Distance protection of transmission lines in presence of inverter-based resources: A new earth fault detection scheme during asymmetrical power swings," IEEE Transactions on Industry Applications, vol. 58, no. 2, pp. 1899-1909, 2022.

[4] A. Chowdhury, S. Paladhi, and A. K. Pradhan, "Nonunit Protection of Parallel Lines Connecting Solar Photovoltaic Plants," IEEE Systems Journal, 2022.

[5] M. N. Uddin, N. Rezaei, and M. S. Arifin, "Hybrid machine learning-based intelligent distance protection and control schemes with fault and zonal classification capabilities for grid-connected wind farms," IEEE Transactions on Industry Applications, 2023.

[6] [6] S. Biswas, P. K. Nayak, B. K. Panigrahi, and G. Pradhan, "An intelligent fault detection and classification technique based on variational mode decomposition-CNN for transmission lines installed with UPFC and wind farm," Electric Power Systems Research, vol. 223, p. 109526, 2023.

[7] H. Teimourzadeh, B. Mohammadi-Ivatloo, and M. Shahidehpour, "Adaptive protection of partially coupled transmission lines," IEEE Transactions on Power Delivery, vol. 36, no. 1, pp. 429-440, 2020.

[8] V. Ashok and A. Yadav, "Fault diagnosis scheme for cross-country faults in dual-circuit line with emphasis on high-impedance fault syndrome," IEEE Systems Journal, vol. 15, no. 2, pp. 2087-2097, 2020.

[9] A. Chowdhury, S. Paladhi, and A. K. Pradhan, "Local positive sequence component based protection of series compensated parallel lines connecting solar photovoltaic plants," Electric Power Systems Research, vol. 225, p. 109811, 2023.

[10] U. Uzubi, A. Ekwue, and E. Ejiogu, "An adaptive distance protection scheme for high varying fault resistances: Updated results," Scientific African, vol. 9, p. e00528, 2020.

[11] Z. Moravej, M. Niasati, and S. H. Mortazavi, "ANN Based Fault Location in Electrical Distribution System," in Power System Protection Conference, iran, 2013.

[12] O. A. Gashteroodkhani, M. Majidi, and M. Etezadi-Amoli, "A fault data based method for zero-sequence impedance estimation of mutually coupled transmission lines," IEEE Transactions on Power Delivery, vol. 36, no. 5, pp. 2768-2776, 2020.

[13] P. D. Raval and A. Pandya, "A hybrid Wavelet-ANN protection scheme for series compensated EHV transmission line," Journal of Intelligent & Fuzzy Systems, vol. 32, no. 4, pp. 3051-3058, 2017.

[14] D. V. Moravej, SP Singh, Zahra, "ANN-based protection scheme for power transformer," Electric Machines & Power Systems, vol. 28, no. 9, pp. 875-884, 2000.

[15] A. Swetapadma, A. Yadav, and A. Y. Abdelaziz, "Intelligent schemes for fault classification in mutually coupled series-compensated parallel transmission lines," Neural Computing and Applications, vol. 32, pp. 6939-6956, 2020.

[16] E. Koley, S. K. Shukla, S. Ghosh, and D. K. Mohanta, "Protection scheme for power transmission lines based on SVM and ANN considering the presence of non‐linear loads," IET Generation, Transmission & Distribution, vol. 11, no. 9, pp. 2333-2341, 2017.

[17] H. Shah, N. Chothani, and J. Chakravorty, "Fault Detection and Classification in Interconnected System with Wind Generation Using ANN and SVM," Advances in Electrical and Electronic Engineering, vol. 20, no. 3, pp. 225-239, 2022.

[18] Z. Moravej, D. Vishwakarma, and S. Singh, "Protection and conditions monitoring of power transformer using ANN," Electric power components and systems, vol. 30, no. 3, pp. 217-231, 2002.

[19] J. C. Quispe Huarcaya, "Transmission line protection challenges infuenced by inverter-based resources: a review," 2022.

[20] G. Ziegler, Numerical distance protection: principles and applications. John Wiley & Sons, 2011.

[21] S. Paladhi and A. K. Pradhan, "Adaptive distance protection for lines connecting converter-interfaced renewable plants," IEEE Journal of Emerging and Selected Topics in Power Electronics, vol. 9, no. 6, pp. 7088-7098, 2020.

[22] Y. Hu, D. Novosel, M. M. Saha, and V. Leitloff, "An adaptive scheme for parallel-line distance protection," IEEE Transactions on Power Delivery, vol. 17, no. 1, pp. 105-110, 2002.

[23] A. Jodaei and Z. Moravej, "Fault Detection and Location in Power Systems with Large-Scale Photovoltaic Power Plant by Adaptive Distance Relays," Iranica Journal of Energy & Environment, vol. 15, no. 3, pp. 265-278, 2024, doi: 10.5829/ijee.2024.15.03.05.

[24] Z. Wang et al., "Intelligent fault detection scheme for constant-speed wind turbines based on improved multiscale fuzzy entropy and adaptive chaotic Aquila optimization-based support vector machine," ISA transactions, vol. 138, pp. 582-602, 2023.

[25] N. R. Babu and B. J. Mohan, "Fault classification in power systems using EMD and SVM," Ain Shams Engineering Journal, vol. 8, no. 2, pp. 103-111, 2017.